

Chapter 9

HIGH-PRESSURE CRYSTAL CHEMISTRY

Charles T. Prewitt

*Geophysical Laboratory and Center for High Pressure Research
Carnegie Institution of Washington
5251 Broad Branch Road, NW
Washington, DC 20015*

Robert T. Downs

*Department of Geosciences
University of Arizona
Tucson, Arizona 85721*

INTRODUCTION

The response of earth materials to increasing pressures and temperatures is an area of research that is of interest to many investigators in geochemistry and geophysics. There have been many scientific pioneers including Bernal, Goldschmidt, Bridgman, Birch, and Ringwood, who made essential contributions to understanding how earth materials combine, disassociate, and transform as environmental conditions change. However, it is only in the past 10-20 years that we have had access to the experimental and theoretical tools that allow us to confirm or dispute the ideas of the pioneers and to make a priori predictions of what will happen when a particular mineral composition is subjected to specific conditions of temperature, pressure, or stress. These developments include new instrumentation for x-ray diffraction and spectroscopy, particularly synchrotron sources, but also new laboratory-based systems with improved x-ray optics and detectors. Neutron scattering sources are built and maintained by national governments, but made available to a wide community of scientists, including earth scientists. Raman, infrared, Brillouin, and Mössbauer spectroscopic techniques have improved substantially, techniques for quantitative chemical and isotopic analysis are accurate and reliable, and powerful digital computers with sophisticated software are available almost everywhere. Thus, we have an astounding array of scientific facilities available to us for, we hope, making astounding discoveries.

The most abundant elements in the Earth are O, Si, Fe, and Mg, and consequently, the most abundant minerals in the Earth contain these elements as major components. As a result, much current research at high pressure involves these elements, the phases they form, and the transitions that take place as we simulate Earth's interior in laboratory apparatus or in computers. The phases of magnesium-iron silicates serve as model systems for studies of high-pressure structures, phase transitions, vibrational dynamics, and chemical bonding. In view of the wide-ranging importance of the high-pressure behavior of oxides, silicates, and sulfides, the literature on this subject is extensive and growing, but far from complete. Recent discoveries include new phases, electronic and magnetic transitions, contrasting results from hydrostatic or differential stress, insight to the role of hydrogen, and how specific phases respond to changing conditions. Thus, there is much new interest in the high-pressure behavior of minerals, with important implications for geology, planetary science, materials science, and fundamental physics. The goal of this chapter is to explore the crystal chemical constraints imposed by the high temperatures and high pressures within the Earth and to provide an overview of the dominant phases

0275-0279/98/0037-0009\$05.00

resulting from mixtures of the major elements under these conditions. We will also discuss the methods used to study crystal structures of minerals under extreme conditions.

An Appendix is included at the end of this chapter that provides the cell parameters, space groups, and atom coordinates for the principal mineral phases of the mantle and core. Although these are parameters derived at ambient conditions, it is felt that they will be useful to those who want to explore the structures more thoroughly using one of the excellent programs now available for displaying and manipulating crystal structures on personal computers.

HIGH-PRESSURE EFFECTS ON BONDING AND COORDINATION NUMBER

Most physical properties of crystalline materials can be understood by examining their crystal structures and the nature of the bonding, i.e. its crystal chemistry. In order to simplify the chemistry and physics involved in high-pressure crystal chemistry we have assembled a set of high-pressure crystal chemical rules of thumb to guide our understanding. Perhaps the starting point for such a set are the rules put forward by Linus Pauling, known as Pauling's Rules. It is assumed that the reader is familiar with these because they are summarized and discussed in most introductory mineralogy texts (see, for example, *Crystallography and Crystal Chemistry*—Bloss 1994).

Rules of thumb

1. *A structure usually compresses by displaying the greatest distortion between atoms separated by the weakest bonds.* Imagine that a crystal structure is composed of spheres separated by springs, each with a given strength, or force constant. In general it is sufficient to assume that the springs exist between nearest neighbors and next-nearest neighbors. For example, within SiO_4 groups in quartz, the nearest neighbor springs are between Si and O and next-nearest neighbor springs are between the six pairs of O atoms. These next nearest neighbor interactions can often be thought of in terms of bond bending. So the O-O springs in SiO_4 tetrahedra are associated with O-Si-O angle bending. A structure usually compresses by displaying the greatest distortion between atoms separated by the softest force constants. In quartz, the force constants can be ranked as stiffest for the SiO bond, then the O-Si-O angle, and weakest for the Si-O-Si angle. Therefore the greatest change in the structure with application of pressure will be the Si-O-Si angles.

2. *Short bonds are the strongest, and long bonds are the weakest.* The force constants between bonded pairs of atoms often can be quickly estimated by examining their separations. Hill et al. (1994) demonstrated that the magnitudes of the bonding force constants in molecules and crystals of nitrides, oxides and sulfides vary in a systematic fashion, with short bonds displaying the largest force constants and long bonds displaying the smallest. The equation for the force constant F_{MX} between a pair of atoms, M and X, is given as:

$$F_{MX} = 7500 \cdot R(MX)^{-5.4} \text{ N/m,}$$

where the bond length, $R(MX)$, is expressed in Ångströms.

3. *As a given bond compresses it becomes more covalent.* This results from the observation that if the distance between a given pair of atoms decreases then the electron density between the atoms must increase in order to keep the bond stable. Gibbs et al. (1994) have shown that such an increase in the electron density between a bonded pair of

atoms comes laterally from the region normal to the bond, and not from along the bond. This makes sense because it is largely the valence electrons that provide the bonding.

4. *Increasing pressure increases coordination number.* Above some point the changes in pressure eventually result in changes in the coordination numbers of the atoms. For example, SiO_4 groups transform to SiO_6 groups with sufficient increase in pressure. An increase in coordination number is usually accompanied by a lengthening of the bonds. For example, $R(\text{Si}^{\text{IV}}\text{O}) = 1.62 \text{ \AA}$ in quartz while $R(\text{Si}^{\text{VI}}\text{O}) = 1.78 \text{ \AA}$ in stishovite. However, the O—O separation usually decreases: it is 2.63 \AA in quartz and 2.51 \AA in stishovite. In addition, the change in coordination number is usually accompanied by an increase in the ionic character of the bond.

5. *The oxygen atom is more compressible than the cations.* Total electron density calculations for coesite and stishovite show that the bonded radius of the oxygen atom decreases by 0.20 \AA while the radius of the Si atoms decreases by 0.02 \AA with the change in coordination from Si^{VI} to Si^{IV} (Nicoll et al. 1994). This is consistent with Pauling's radius ratio rule. For the coordination number of Si to increase from 4 to 6 requires that the ratio of $r(\text{Si})/r(\text{O})$ increase. This can occur only if $r(\text{O})$ decreases relative to $r(\text{Si})$. The reason that oxygen is more compressible than the cations is not related to the size of the atoms but rather to the slope of the electron density in the bonding region. The electron density of oxygen falls off rather rapidly compared to the electron densities around cations, which fall off slowly. Therefore, as a bond is compressed and shortened it appears that the size of the oxygen shrinks relative to the cation.

6. *Angle bending is dependent upon coordination.* Little is known about angle bending force constant systematics. For example, molecular orbital calculations show that Si-O-Si angles are stiffer than Si-O-Al but weaker than Si-O-B (Nicholas et al. 1992). This observation may be related to the distance between cations as discussed earlier in rule #2. However, we also know that if a bridging oxygen atom is coordinated to yet a third atom then the force constant of the angle increases dramatically (Geisinger et al. 1985). Such effects are observed while compressing framework structures such as the feldspar minerals and may also be related to garnet compressibility systematics.

7. *O-O packing interactions are important.* Inter-tetrahedral O-O interactions are known to be very important in understanding the compression of silica framework structures. For example, work by Lasaga and Gibbs (1987) and Boisen and Gibbs (1993) using force field calculations could not replicate experimental compression behavior for silica polymorphs unless strong O-O repulsion terms were included in the energy calculations. All first principles and ionic model calculations include the O-O interactions implicitly, but little systematic work has been done to quantify the magnitude of its importance. For instance, olivines are closest-packed structures and yet the compressibility has been studied in terms of the bonding in the octahedral and tetrahedral sites. It may be that its compressibility is determined principally by O-O interactions.

8. *High-pressure structures tend to be composed of closest-packed arrays of atoms.* Application of pressure on a crystal structure forces the atoms to occupy a smaller volume. Closest-packed structures are the densest arrangement of atoms and therefore high-pressure structures tend to be composed of closest-packed arrays of atoms. For oxide minerals this means that the structures found deep in the Earth are generally closed-packed arrays of oxide atoms, with short-ranged metal-oxygen bonding perturbing the arrangement. Pressure forces the oxygen atoms into more regularly close-packed arrangements, but the cation-oxygen bonds influence how they get there. For example, in their study of kyanite, Yang et al. (1997) found that the arrangement of oxygen atoms became more closest-packed under pressure. They computed a best fitting ideal closest-packed array of oxygen

atoms to the observed structure as a function of pressure by minimizing the distance between the observed atomic positions and those in the ideal array by varying the radii and orientation of the ideal array. The result produced a value for the radius of oxygen and an isotropic root-mean square displacement parameter that describe the deviation of the structure from ideal. They found that the oxygen atoms became more closest-packed, with $U_{\text{iso}} = 0.0658 \text{ \AA}$ at room pressure and $U_{\text{iso}} = 0.0607 \text{ \AA}$ at 4.5 GPa. Furthermore the radius of the oxygen atom decreases from 1.372 \AA to 1.362 \AA . The compression was anisotropic, with the most compressible direction oriented parallel to the direction of the closest-packed planes that were furthest apart. Another example is quartz, SiO_2 . Quartz traditionally represents the prototype framework structure with its corner-linked SiO_4 groups and is never called a closest-packed structure. Yet as pressure is applied the O atoms tend to arrange themselves in closest packed layers, oriented parallel to (1 20) (Hazen et al. 1989).

9. Elements behave at high pressures like the elements below them in the periodic table at lower pressures. For example, at high pressure Si behaves like Ge does at low pressure. Because of this observation, many studies of germanate compounds have been conducted as high-pressure silicate analogues in days past because sufficiently high-pressure experimental conditions were unattainable. The germanates tend to display structures that are similar to silicates and undergo similar phase transformations at more modest pressures. This can also be understood in terms of softer anions with Pauling's radius ratio rule. Upon application of pressure to, say a SiO_4 group we see that the $r(\text{O})$ decrease at a faster rate than the $r(\text{Si})$ and so $r(\text{Si})/r(\text{O})$ increases. However, at ambient conditions $r(\text{Ge}) > r(\text{Si})$ so the ratio of $r(\text{Ge})/r(\text{O})$ is already greater than for Si-O. This rule of thumb may also apply to oxygen and sulfur inasmuch as sulfides at room pressure appear to behave like oxides at high-pressure. For example, it is known that S-S bonding in sulfides is prevalent, e.g. pyrite. Recent work has shown that at high pressures O-O bonding can be found in low quartz (Gibbs et al., submitted).

As with many rules of thumb, ours are not laws of nature because the behavior of crystalline materials can often be quite complicated. These rules are provided as a guide of what first to think about when pressure is applied. Departures from the rules often can indicate the presence of multiple interactions, which are, of course, the most exciting to investigate. For every one of these rules of thumb we could probably find an exception. For example, GeO_2 does not crystallize with the coesite structure. Even though closest packing is the most efficient way to pack atoms, many elemental phases (such as Pb) convert to a body-centered structure at high-pressure. Ideal MgSiO_3 perovskite is cubic and can be regarded as composed of a closest-packed array of O and Mg with Si in the octahedral voids. However, it actually is found to be orthorhombic, with distorted closest packing, which deviates even more with pressure. The reasons are interesting, and can be related to the differences in the force constants between O-O, Si-O and Mg-O.

COMPARATIVE COMPRESSIBILITIES

When analyzing the behavior of a crystal structure with changes in pressure, it is useful to understand how the relative sizes of atoms (ions) change. Measurements of the change of a unit cell as pressure increases can be obtained rather easily. However, it is more difficult to determine the change in individual ions, not only because of experimental difficulties, but also because assumptions have to be made about whether the changes take place in cations or anions, or both. There has been extensive discussion in the scientific literature about how one defines the radius of a cation or anion, ranging from empirical assignments of a specific radius to oxygen ions (Shannon and Prewitt 1968), to relatively sophisticated molecular orbital calculations (Nicoll et al. 1994). Except for structures with no variable atom coordinates (e.g. NaCl), information on compression of interatomic

distances has to be obtained from accurate crystal structure determinations as a function of pressure (and/or temperature).

In general, compressibility of a cation or an anion is proportional to the size of the ion and the coordination number, and inversely proportional to the charge on the ion. Thus, eight-coordinated Na^+ is much more compressible than tetrahedrally-coordinated Si^{4+} . The systematics of ionic compressibility are described in detail by Hazen and Finger (1979, 1982). They give the relation (converted from Mbar to GPa)

$$\frac{K_p d^3}{z_c} = 750 \pm 20 \text{ GPa-}\text{\AA}^3$$

where K_p is the polyhedral bulk modulus in GPa d is the mean cation-anion distance in \AA , and z_c is the integral formal charge on the cation. The polyhedral bulk modulus is obtained by calculating the volume of two coordination polyhedra in a structure at different pressures and using

$$K_p = -\frac{(V_1 + V_2)}{2} \left(\frac{\Delta P}{\Delta V} \right)$$

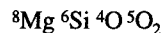
where $(V_1 + V_2)/2$ is the average volume of the two polyhedra being compared. This relation can provide semiquantitative insight into how different cation polyhedra will behave under compression, but it should be noted that the assumption here is that the concept of macroscopic ("continuous") moduli can be transferred to the atomic scale.

MECHANISMS OF PHASE TRANSITIONS

One of the more interesting aspects of crystal chemistry at high pressures and temperatures involves phase transitions that are accompanied by changes in physical and chemical properties of the phases involved. Phase transitions are very important in studies of Earth's interior because they involve changes in elastic properties and densities of minerals that can be detected via the analysis of seismic waves created by earthquakes and thus provide information about the inner structure of the Earth. One goal of mineral physics investigations is to study relevant phase changes in the laboratory and to attempt to understand why they take place under specific conditions of pressure, temperature, and varying composition.

From a crystal structural point of view, phase transitions are generally described as *reconstructive* or *displacive*, and from a thermodynamic perspective as *first-order* or *second-order* (Buerger 1961). The fundamental definition of a reconstructive transition involves breaking of bonds and can range from a relatively subtle change in a structure to a very drastic one. In contrast, a displacive transition is one that does not involve breaking of existing bonds and creation of new ones, but only involves a shifting of the atomic positions, possibly with a symmetry change. It is incorrect to equate reconstructive with first-order and displacive with second-order, because there are examples where differences are subtle and it is not possible to make such comparisons. There are, for example, displacive transitions that are accompanied by discontinuities in lattice parameters, which indicates that they are also first-order transitions. Other descriptions of phase transitions include *martensitic* (one involving a tilt or distortion of the structure and mostly applied to metals and alloys) and *soft mode* (where one or more modes in, say, a Raman spectrum disappear at the transition). A more complete discussion of phase transition theory is not warranted in this chapter, but the reader should be aware that these categories do exist and are discussed extensively in the literature.

A major aspect of high-pressure phase transitions is the increase in cation and anion coordination as a function of increasing pressure. Emphasis is usually placed on changes in cation coordination, but anion coordination must also increase, as described by the formula for magnesium silicate perovskite:



Thus, the total coordination of the cations is $8 + 6 = 14$, and for oxygen is $4*1 + 5*2 = 14$. This relation holds for all phase transitions and it should be noted that in some structures crystallographically-different oxygens or other anions may have different coordination numbers. Shannon and Prewitt (1968) showed that as coordination of an ion increases, the average interatomic distances to that ion also increase, an apparent paradox for a transition where the density of the high-pressure phase is always higher. It works out satisfactorily, however, because the ions in the high-pressure phase must always be packed together more efficiently. Several other examples for MgSiO_3 phases are

Enstatite	${}^6\text{Mg } {}^4\text{Si } {}^3\text{O}_2 \text{ }^4\text{O}$	$6*1 + 4*1 = 3*2 + 4*1$
Majorite	${}^8\text{Mg}_3 \text{ }^6(\text{MgSi}) \text{ }^4\text{Si}_3 \text{ }^4\text{O}_{12}$	$8*3 + 6*2 + 4*3 = 4*12$
Ilmenite	${}^6\text{Mg } {}^6\text{Si } {}^4\text{O}_3$	$6*1 + 6*1 = 4*3$

One other feature related to coordination number is the geometrical relation of the coordinating ions to each other. In high-pressure phases the four- and six-coordinating groups almost always form tetrahedra or octahedra. Five-coordinated cations are relatively unusual although one Al site in andalusite can be described as a trigonal bipyramid and Angel et al. (1996) and Kudoh et al. (1998) reported that a phase transition in CaSi_2O_5 at about 0.2 GPa results in five-coordinated Si. In MgSiO_3 perovskite, oxygen is coordinated by three Mg and two Si in a rectangular pyramid with two Mg and two Si forming the base and the other Mg at the apex. The Mg coordination in this structure is sometimes referred to as dodecahedral (Poirier 1991), but it is perhaps better described as a bicapped trigonal prism with the six closest oxygens forming a trigonal prism and the next two closest oxygens positioned outside two of the prism faces. In contrast to the one in perovskite, the polyhedron around Mg in majorite is a slightly distorted triangular dodecahedron with eight vertices and twelve triangular faces. There are, of course, other geometrical arrangements in high-pressure phases, but these are the ones most common in mantle phases.

ANALYTICAL TECHNIQUES

X-ray diffraction is the most important analytical tool used to gain information on the crystallographic properties of high-pressure phases. The approach used to learn about the crystal chemistry of high-pressure, high-temperature phases depends on the objectives of the investigation and upon the tools available. For example, much information can be derived from examination of quenched high-pressure phases if the material in question retains the high-pressure structure upon quench. However, there are limitations to this approach, including the fact that the unit cell and interatomic distances in a quenched phase are different from the ones in the material before the quench. Furthermore, it is always possible that the symmetry and/or crystal structure undergo significant changes upon quench even though the material remains crystalline—in many examples single crystals remain single through one or more phase transitions as external conditions are varied.

For in situ single-crystal diffraction experiments at high pressures and/or high temperatures, the most common device used to apply pressure is the Merrill-Bassett (Merrill and Bassett 1974) diamond-anvil cell. This cell employs a simple clamping mechanism to push together two brilliant-cut diamonds that are positioned on either side of a hole in a metal gasket that contains the crystal being studied. The crystal is suspended in a pressure

medium that is usually a mixture of ethanol and methanol, although other organic liquids, water, or cryogenic liquids of noble elements such as neon, argon or helium are sometimes used when loading a diamond cell. In order to provide as large an opening for incident and diffracted x-rays as possible a beryllium disk that is relatively transparent to x-rays backs each diamond. One disadvantage of this is that the resulting polycrystalline diffraction pattern and associated diffuse scattering from beryllium must be accounted for in the data analysis. Using this approach pressures up to 10 GPa can be obtained to record good-quality single-crystal intensity data on a routine basis; pressures as high as 33 GPa have been reported (Zhang et al. 1998).

Applying simultaneous elevated pressures and temperatures for a single-crystal experiment is more difficult than for either pressure or temperature alone. Heat is generally applied with resistance wire wrapped around the diamonds and temperatures to about 600°C can be reached. Because beryllium and other metals weaken at high temperatures and because beryllium oxide vapor is poisonous, investigators have generally used other materials for the backing disk. One such material is B₄C, which is a ceramic that transmits x-rays, but is brittle and will crack and break at pressures higher than about 2-4 GPa.

Some of the above limitations may be overcome with the growing use of synchrotron radiation for high-pressure work. There have been relatively few high-pressure single-crystal experiments conducted at synchrotron x-ray sources [examples are by Mao and Hemley (1996) on stishovite at 65 GPa and by Loubeyre et al. (1996) on H₂ crystals at 119 GPa], and even fewer that involved recording of accurate diffraction intensities for structure determinations or refinements. However, the production of shorter x-ray wavelengths at synchrotrons, improvements in beam stability, and increasing availability of area x-ray detectors capable of recording high-energy radiation make such investigations appear feasible. The shorter wavelengths make it possible to collect sufficient diffraction data in a more restricted angular range of incident and diffracted x-ray beams. In the future this may allow the construction of diamond cells that do not require beryllium backing disks. Diamonds can be mounted directly on tungsten carbide plates having conical apertures for the x-rays to enter and leave the cell. Not only will this decrease the background x-ray scattering, it should also permit inclusion of resistance heaters to provide temperatures up to at least 800°C.

Powder x-ray diffraction

In contrast to single-crystal investigations at high pressure, there have been relatively few powder structure determinations at high-pressure using conventional laboratory apparatus. For many years, high-pressure powder diffraction experiments were confined to recording changes in cell parameters and detecting the occurrence of phase transitions because the only available diffraction tools were sealed-tube x-ray generators and film or scintillation detectors that resulted in inefficient recording of diffraction patterns. In the past 10 years however, new developments in x-ray optics, x-ray generators, synchrotron x-ray sources, detectors, computer control, and analytical software have changed the situation drastically. Improved diamond cells and the ability to reduce the amount of sample required (~10 μm) because high-intensity micro x-ray beams can be focused to the same size as the sample result in the ability to obtain good diffraction patterns on polycrystalline samples at pressures in the 1-3 megabar range. Although most of these kinds of experiments are now being done at synchrotron sources, Hasegawa and Badding (1997) showed that it is possible to collect satisfactory data with a laboratory rotating-anode generator, an x-ray monochromator, and x-ray film as a detector. With further developments of focusing optics, x-ray generation, and either imaging plates or CCD (charge-coupled device)

detectors, it is likely that more investigators will make serious attempts to improve their "conventional" laboratory facilities.

Synchrotron radiation sources

Since the "second-generation" synchrotron sources became available to mineral physicists in the early 1980s, there has been strong interest in using these machines for investigations at high pressure. Fundamentally, there are two distinctly different kinds of experiments that are of interest, one uses polychromatic or "white" x-radiation and the other monochromatic x-radiation. There are advantages and disadvantages to each. White radiation experiments take advantage of the continuous x-ray spectrum produced by a synchrotron such as the one at the National Synchrotron Light Source, Brookhaven National Laboratory. In this kind of experiment, a powder sample is held in a diamond cell that has relatively small angular ports for incident and diffracted x-rays and the detector is placed to record the diffracted pattern. One kind of detector is a "point" detector that measures x-rays at a given angle from the direct beam. A common point detector is a solid-state Ge detector that can record a wide energy range and thus records the x-ray spectrum of intensity as a function of energy. Neither the sample nor the detector has to move during an experiment, but changes in cell parameters and the occurrence of phase transitions are measured easily. A major disadvantage is that it is difficult to impossible to make quantitative use of the diffraction intensities because there are so many poorly defined variables in such experiments. Another problem with the second-generation synchrotron sources is that their x-ray intensities decrease substantially as energy increases toward the values most useful for transmission through the diamond cell. A solution is to use a "wiggler" port at the synchrotron that produces a higher energy x-ray spectrum. Such ports are available at NSLS, the Photon Factory, and SSRL.

Three "third-generation" synchrotron sources were built in the 1990s and are now available for use by high-pressure scientists. These are the European Synchrotron Radiation Facility (ESRF) in Grenoble, France, the Advanced Photon Source (APS) at Argonne National Laboratory in Illinois, and SPring-8 near Aoki, Japan. The advantage of all these machines is that they produce high-energy x-rays from their standard bending magnets and are further enhanced by the use of insertion devices, i.e. undulators and wigglers, that boost the x-ray energies to even higher values. A variety of high-pressure experiments are being pursued at all these facilities, including diamond-cell energy dispersive experiments with white radiation, monochromatic diamond-cell experiments, and experiments with large-volume, multi-anvil apparatus.

Neutron powder diffraction

A few papers have been published on the use of powder neutron diffraction to obtain crystal-chemical data on mineral structures at high pressure. Most of the experiments described in these papers utilized neutrons rather than x-rays because the locations of hydrogen or deuterium atoms in hydrous phases can be found more easily. Negative aspects of neutron diffraction are that it requires more sample than does x-ray diffraction and most of the high-pressure cells designed thus far are limited to pressures less than about 10 GPa, but there are attempts to increase this limit to at least 20 GPa. The pressure cell most widely used for neutron is the Paris-Edinburgh cell designed by Besson (Besson et al. 1992). The primary neutron sources used for experiments with this cell are the Los Alamos Neutron Science Center (LANSCE) at Los Alamos National Laboratory in New Mexico and the pulsed neutron source (ISIS) at the Rutherford-Appleton Laboratory in the United Kingdom.

In addition to locating and refining hydrogen/deuterium atoms with neutrons, another goal has been to investigate how the H-O distances change with pressure. Hydrogen bonds in oxides including silicates are generally in the form O-H...O where the O-H distance is ~ 0.95 Å, the H...O distance is about 2.3 Å, and the O-H...O angle is in the 160° - 170° range. The O-D...O distances and angles are slightly different when D substitutes for H in the same crystal structure. In their study of brucite, $\text{Mg}(\text{OD})_2$, to 9.3 GPa, Parise et al. (1994) found that the O-D distance did not change with pressure, but that D became disordered into three equivalent positions around the threefold axis in the trigonal space group and the D...O distance decreases from 2.291 Å at 1 atm. to 1.95 Å at 9.3 GPa. There was no observable change in the overall symmetry.

In another application of neutron diffraction, Lager and Von Dreele (1996) used ISIS to collect data on the hydrogarnet katoite $[\text{Ca}_3\text{Al}_2(\text{O}_4\text{D}_4)_3]$ at several pressures up to 9.0 GPa. In this example, the O-D distance decreased from 0.906 Å at one atm. to 0.75 Å at 9 GPa, while the O...D distance decreased from 2.54 Å to 2.48 Å. At the same time, the O-D...O angle increased from about 137° to 141° . Clearly, it is important to obtain more data on different structures so that it will be possible to develop a coherent picture of hydrogen bonding in oxide minerals at high pressure.

HIGH-PRESSURE PHASES

This section provides information about the major and some of the minor phases that are important in determining the character of Earth's inner core, the lower mantle, the transition zone, and the upper mantle. It is a discussion of crystal-chemical concepts and current research directions that investigators believe are important in directing high-pressure experiments and interpreting the results. We have made no attempt to review every detail for each phase involved, but instead try to give the reader an overview of high-pressure mineralogy and hope that this will encourage further research on a wide range of topics. In contrast to the usual approach of starting with Earth's crust and working downward, we first look at the possible mineralogy of the inner core and proceeding upward from there. This approach is used because the high-pressure phases are generally more simple than low-pressure phases, in that they always adopt some sort of closest packing scheme.

In order to set the stage for describing each major mineral phase in the lower and upper mantles, Figure 1 is a phase diagram from Gasparik (1993) that shows both hydrous and anhydrous magnesium silicates that occur in the mantle. When reading through the various mineral descriptions below, the reader can refer to this diagram to see the pressure-temperature regions where the particular phase is stable.

Iron

At ambient conditions Fe adopts a body-centered cubic (bcc) structure (α -Fe). However, at high temperatures it transforms to γ -Fe, a face-centered cubic, closest-packed structure (fcc), and at high pressures it becomes hexagonal closest-packed (hcp), ϵ -Fe. There is a major controversy about yet another possible phase (Boehler 1990, Saxena et al. 1993) that is designated as β -Fe and appears above about 1000 K and 100 GPa. A group at Uppsala University (Saxena et al. 1995, Dubrovinsky et al. 1997) maintains that this phase exists and has a dhcp structure, meaning that the closest-packed monolayers are arranged as *abacaba*, thereby effectively doubling the *c* cell edge. Other investigators from the Carnegie Geophysical Laboratory (Shen et al. 1998) did not observe evidence for phases other than ϵ -Fe or γ -Fe in situ, but state that the diffraction patterns of temperature-quenched products at high pressure could be fit to other structures such as dhcp. The reason that this is important is that the proposed pressure-temperature range proposed for the possible β -Fe includes the conditions present in Earth's inner core. Thus, definitive

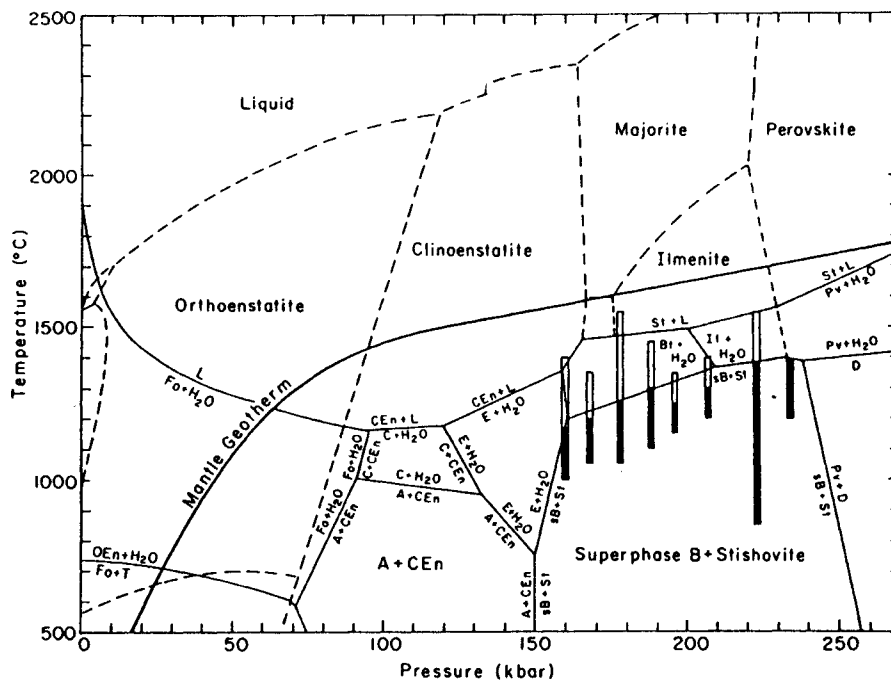


Figure 1. Temperature-pressure phase diagram from the system $\text{MgO-SiO}_2\text{-H}_2\text{O}$ (solid lines). Dashed lines are phase boundaries in the anhydrous MgSiO_3 system. This diagram demonstrates the effect of H_2O on phase relations. [Used by permission of the editor of *Journal of Geophysical Research*, from Gasparik (1993), Fig. 5, p. 4294.]

knowledge of the crystal structure of iron in the inner core could be essential for understanding its physical properties such as the anisotropy of transmission of seismic waves through the core. Anderson (1997) gives an interesting discussion of the various points of view on this controversy.

Magnesiowüstite

At ambient conditions both FeO (wüstite) and MgO (periclase) adopt the cubic closest packed structure of rock salt (Fig. 2). This structure can be envisioned as a stacking of closest packed monolayers along the $[111]$ direction. However, at high pressures FeO undergoes several phase transitions whereas MgO does not. The phase believed to occur in

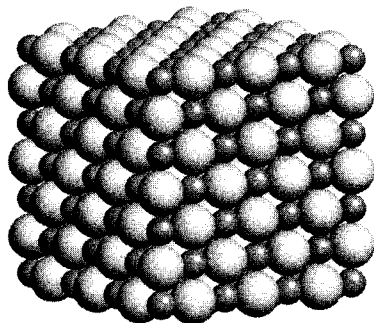


Figure 2. Structure of magnesiowüstite illustrating cubic closest packing of anion and cation layers. The sizes of the atoms are chosen only as a guide to aid in visualization.

the lower mantle is called magnesiowüstite by many investigators, but it actually should be called ferropericlaase because all models of the lower mantle assume only 10-20% Fe. However, magnesiowüstite seems to be the dominant terminology for intermediate compositions and we will continue that usage here. In addition, some of the most interesting crystal chemistry results from experiments on FeO at high pressure where it transforms to a NiAs-type structure. However, some high-pressure experiments have been performed on magnesiowüstite such as those by Shu et al. (1998) where intermediate compositions up to $(\text{Fe}_{0.60}\text{Mg}_{0.40})\text{O}$ underwent phase transitions between 25 and 40 GPa at room temperature, but no transition was observed for $(\text{Fe}_{0.40}\text{Mg}_{0.60})\text{O}$ up to 48 GPa. Thus, it is not clear whether or what transitions can be expected for magnesiowüstite compositions of the lower mantle.

Using shock wave and diamond-cell techniques, Jeanloz and Ahrens (1980) and Knittle and Jeanloz (1986) reported a phase transition in FeO at about 70 GPa and temperatures exceeding 1000 K. Knittle and Jeanloz interpreted the shock wave results as evidence for a change in ferrous iron character at high pressures, resulting in a metallic phase. However, they found no such evidence in resistivity measurements in the diamond cell. Zou et al. (1980) and Yagi et al. (1985) found that at low temperature and at pressures above 20 GPa, FeO undergoes a rhombohedral distortion (rhombohedral angle $<60^\circ$), which increases with pressure. The distortion results in a shortened Fe-Fe distance. The results of first-principles LAPW calculations (Isaak et al. 1993) show that the distortion originates with the onset of Fe-Fe bonding, which has some covalent character and results in a decrease in the interplanar Fe-Fe distances. The magnitude of the Fe-Fe interactions increases with pressure, causing an increase in the rhombohedral distortion (Mazin and Anisimov 1997a). With application of even more pressure a phase transition into a hexagonal structure was observed (Fei and Mao 1994) at high temperatures (600 K at 96 GPa) which was interpreted to be a NiAs-type (B8) structure, the hexagonal analogue of the rocksalt structure. In other words, the transition investigated by Fei and Mao represents a change of symmetry due to a different stacking sequence of the close-packed planes, with the nearest-neighbor Fe-O distances being essentially the same in both structures. In a subsequent development, it was discovered that diffraction patterns of the structure regarded as B8 actually has diffraction intensities consistent with a structure containing both B8 and anti-B8 domains. In the anti-B8 structure, Fe and O are exchanged between non-equivalent crystallographic sites, where Fe has trigonal prismatic and O has octahedral coordination (Mazin et al. 1998).

Perovskite, ilmenite

Perovskite is a mineral with the composition CaTiO_3 and originally was thought to be cubic with Ca coordinated by 12 oxygens in a cubo-octahedral geometry and Ti in an octahedron. Further work showed that it is actually orthorhombic and that Ca is coordinated by eight oxygens. It is difficult to know who was the first scientist to realize that MgSiO_3 enstatite or Mg_2SiO_4 olivine might transform to the perovskite structure at high pressure, but it was mentioned as a possibility by Ringwood (1962), and Ringwood and Major (1967a) synthesized germanates with the orthorhombic perovskite structure, which was possible with an existing high pressure apparatus. In the first successful experiment on a silicate, Liu (1974) obtained silicate perovskite by starting with pyrope ($\text{Mg}_3\text{Al}_2\text{Si}_3\text{O}_{12}$) and laser-heating it in a diamond-anvil cell at 27-32 GPa to produce MgSiO_3 perovskite plus corundum. Investigators soon realized that silicate perovskite could be the dominant phase in the lower mantle and, if so, the most abundant mineral in the Earth. The structure of orthorhombic silicate perovskite is shown in Figure 3.

Today, silicate perovskite is synthesized easily in diamond cells and in large-volume,

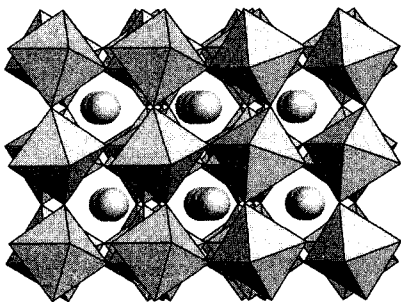


Figure 3. Structure of orthorhombic perovskite viewed down [110]. The SiO_6 groups are illustrated as octahedra, with Mg illustrated as a sphere.

multi-anvil apparatus at pressures of 22 GPa and above. Single crystals as well as powder samples have been made and the crystal structure and elastic properties determined by several different investigators. There have, however, been arguments about the range of stability of perovskite at high temperatures and whether it might break down into MgO and SiO_2 under conditions existing in the lower mantle (Saxena et al. 1996). This was disputed by Mao et al. (1997) and Serghiou et al. (1998), and the exact conditions required for perovskite stability is still an open question. Fei et al. (1996) presented a diagram showing that there is a maximum amount of Fe^{2+} that $(\text{Mg,Fe})\text{SiO}_3$ perovskite can accommodate at any given pressure and temperature (see Fig. 6 in Fei, this volume). Mao et al. (1997) and McCammon (1998) found that $(\text{Mg,Fe})\text{SiO}_3$ perovskite synthesized in both diamond cells and multi-anvil presses contain a significant amount of Fe^{3+} that can stabilize the structure. This also implies that Al^{3+} can have the same effect and that the amount of Fe^{3+} and Al^{3+} in the lower mantle will have a strong influence on the range of stability of perovskite. It is clear that research on this general subject will continue for the foreseeable future.

No natural samples of silicate perovskite from the lower mantle have been reported although some workers have predicted that it might be found as an inclusion in diamond. However, there are two recent reports of $(\text{Mg,Fe})\text{SiO}_3$ ilmenite and more limited evidence for the presence of perovskite in shocked meteorites (Sharp et al. 1997, Tomioka and Fujino 1997). It remains to be seen whether the evidence is strong enough for either of these phases to be approved for official mineral names by the International Mineralogical Association. The ilmenite structure is a derivative of the corundum structure except that it consists of two crystallographically-distinct octahedra, each occupied by Mg and Si, respectively, and is shown in Figure 4.

Stishovite, coesite, quartz

An extensive discussion of silica minerals at high pressure is available in Hemley et al. (1994). Therefore, only a brief summary of the two high-pressure silica phases, stishovite and coesite, is given here.

Stishovite (Fig. 5) is the highest-pressure form of SiO_2 that has been found as a mineral, i.e. in shocked siliceous rocks resulting from meteorite impacts. Stishovite has the rutile structure with Si in octahedral coordination and the octahedra forming edge-shared chains along the c axis that are each connected to four other parallel chains. The crystal structure as a function of pressure has been determined by Sugiyama et al. (1987) to 6 GPa and by Ross et al. (1990) to 16 GPa. It was observed that the compression is anisotropic with the a axis almost twice as compressible as the c axis. The structural response to compression can be considered as mainly polyhedral tilting along with some compression of the SiO bonds, but without appreciable distortion of the octahedra. It came as a surprise that the shared edge O-O separations were not the least compressible. In contrast with earlier workers (Megaw 1973), we find that stishovite can effectively be considered a

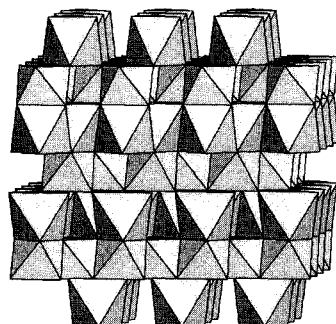


Figure 4. Structure of ilmenite viewed along the *ab* plane showing alternating planes of non-equivalent octahedral layers.

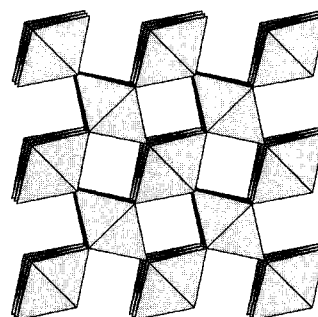


Figure 5. Structure of stishovite viewed down the *c* axis. Note the distorted closest-packed layers of O atoms that align with the edges of the octahedra.

distorted hexagonal closest-packed array of O atoms with Si in octahedral voids. The shared edges of the octahedra ensure distortion. With increasing pressure the O atoms become more closely packed, accounting for the distribution in O-O compression systematics.

A post-stishovite phase with the CaCl_2 structure was confirmed experimentally in high-pressure x-ray (Tsuchida and Yagi 1989) and Raman (Kingma et al. 1995) experiments. The latter study also examined the temperature dependence of the transition using calculations based on the potential induced breathing model (PIB++) and concluded that any free silica in the lower mantle would have the CaCl_2 structure above about 60 GPa. This structure involves a slight tilting of the SiO_6 octahedra, no breaking of bonds, and a symmetry change from the tetragonal space group $P4_2/mnm$ to orthorhombic $Pnmm$. The polyhedral tilting observed in the transformation to the CaCl_2 structure demonstrates that the closest-packing layers should be considered stacked along the *b*-axis direction. Theoretical electron density maps for stishovite at pressure constructed by Gibbs et al. (1998) suggest that the CaCl_2 transformation is coincident with the onset of O-O bonding.

Several other post-stishovite phases have been proposed and Teter et al. (1998) describe the various possibilities based on crystal chemical reasoning and first-principles total-energy calculations. Using a laser-heated diamond cell at pressures up to 85 GPa, Dubrovinsky et al. (1997) synthesized a silica phase identified as intermediate between the *a* PbO_2 and ZrO_2 (baddelyite) structures, and El Goresy et al. (1998) found a phase in the shocked SNC meteorite Shergotty whose diffraction pattern is consistent with that of a silica phase with the ZrO_2 structure. The ultimate high-pressure phase of SiO_2 , the cubic phase with the $P\bar{a}3$ space group, similar to the pyrite structure, has not yet been reported.

Coesite represents the highest-pressure stable polymorph of the tetrahedrally coordinated silica phases (Fig. 6). It forms a structure that in some ways is similar to that of the feldspars. Four membered rings of tetrahedra form chains that run parallel to the *c*-axis. These chains lie on layers that are perpendicular to *b* with a channel separating each chain. Each layer is shifted over the adjoining layers in such a way that chains are always over channels. This is the fundamental way that the framework structure of coesite differs from feldspar. An important feature of the crystal structure that has received much attention is an apparent linear Si-O-Si angle. The nature of this angle has been a subject of considerable debate because the equilibrium Si-O-Si angle is around 144° .

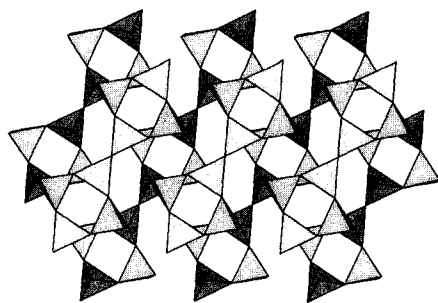


Figure 6. Structure of coesite viewed down the *b* axis. Two layers of the chains of 4-membered tetrahedral rings are displayed. The chains run parallel to the *c* axis.

Levien and Prewitt (1981) determined the crystal structure of coesite as a function of pressure. They demonstrated that the compressibility of coesite is quite anisotropic, with the stiffest direction parallel to the chains and the softest direction coincident with narrowing the widths of the channels. All Si-O-Si angles decrease except for Si1-O1-Si1, which is constrained to be 180°. However, all temperature factors decrease with application of pressure except for O1, which increases significantly. Such an increase is consistent with a bent Si-O-Si angle in which the O1 atom is librating under toroidal motion. Increasing pressure would bend the angle further, thus effectively increasing the temperature factor.

Other metastable high-pressure silica phases have been observed in experiments using coesite (Hemley et al. 1988, Williams et al. 1993), cristobalite (Tsuchida and Yagi 1990, Downs and Palmer 1994, Palmer et al. 1994), and quartz (Kingma et al. 1996) as starting materials. As these are not likely to be significant mantle phases, they are not discussed further here. Those interested should consult Hemley et al. (1994).

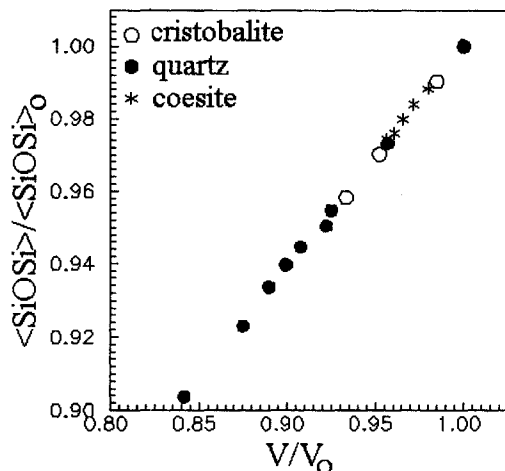


Figure 7. Normalized unit cell volume, V/V_0 , vs the normalized average Si-O-Si angle, $\langle \text{Si-O-Si} \rangle / \langle \text{Si-O-Si} \rangle_0$ for quartz, coesite, and cristobalite.

The compression of the tetrahedral silica polymorphs is controlled by the compression of the Si-O-Si angle. Figure 7 shows a plot of the normalized unit cell volume, V/V_0 , versus the normalized average Si-O-Si angle, $\langle \text{Si-O-Si} \rangle / \langle \text{Si-O-Si} \rangle_0$, for quartz, coesite and cristobalite (Glennemann et al. 1992, Levien et al. 1980, Levien and Prewitt 1981,

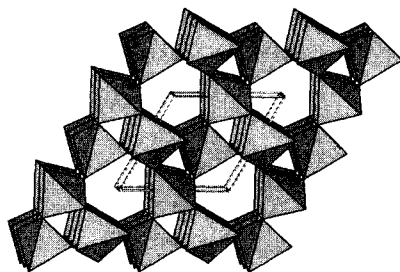


Figure 8. Quartz structure viewed down the c axis.

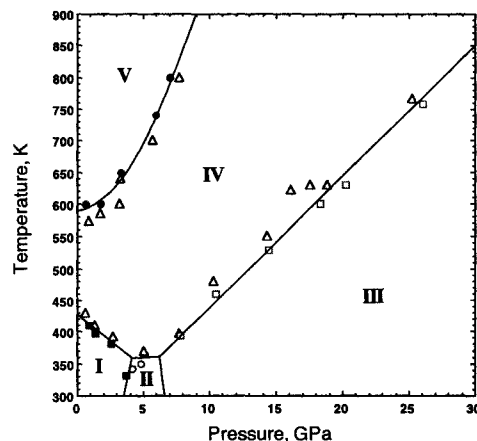


Figure 9 (right). Experimentally determined phase diagram of FeS. FeS I, NiAs-type structure with a $(\sqrt{3}a, 2c)$ unit cell; FeS II, MnP-type structure; FeS III, monoclinic; FeS IV, NiAs-type structure with a $(2a, c)$ unit cell; FeS V, NiAs-type structure with a (a, c) unit cell. [Used by permission of the editor of *Science*, from Fei et al. (1995), Fig. 2, p. 1893.]

Downs and Palmer 1994, Hazen et al. 1989). The figure demonstrates that the compression of each of the three structures is controlled in the same way by the angle. The structure of quartz is shown in Figure 8.

FeS

Iron and sulfur are important components of the interiors of the terrestrial planets and it is possible that a high-pressure phase of FeS is present in Earth's lower mantle and the inner core. Under ambient conditions, FeS has the troilite structure (FeS I), but with increasing pressure and/or temperature it undergoes phase transitions to either more symmetric (with temperature) or more distorted (with pressure) structures. Figure 9 is the phase diagram of FeS from Fei et al. (1995) and shows that FeS I transforms to FeS II with the MnP structure at room temperature and 3.5 GPa and to FeS III at about 6.5 GPa. The structure of FeS III was reported by Nelmes et al. (1998) and refinements of FeS IV and V by Fei et al. (1998). These structures are all similar to each other and based on distortions of the hexagonal NiAs structure, except for FeS V, which has the NiAs structure. This structure is based on layers of edge-shared FeS_6 octahedra in which each octahedron shares faces with octahedra in parallel layers above and below. This results in rather short Fe-Fe distances and is important in determining the electronic and magnetic properties of these phases. The Fe atoms form a trigonal prism around each sulfur atom. Figure 10 shows the structures of FeS II (A) and FeS III (B). Note that in FeS II the octahedra are relatively symmetric; by contrast the octahedra in FeS III are highly distorted.

Garnet

Garnet, primarily pyrope and majorite, is an important component in the upper regions of the Earth, accounting for up to 10% of the volume of the upper mantle, and up to 50% of the transition zone (Ita and Stixrude 1992). The chemical formula of garnet can be written $A_3B_2(\text{SiO}_4)_3$, with pyrope as $\text{Mg}_3\text{Al}_2(\text{SiO}_4)_3$ and majorite as $\text{Mg}_3(\text{Mg, Si})_2(\text{SiO}_4)_3 = \text{MgSiO}_3$. The structure (Fig. 11) can be viewed as a rather rigid framework of corner sharing octahedra (B -site) and tetrahedra, with the A -site atom located in interstices that

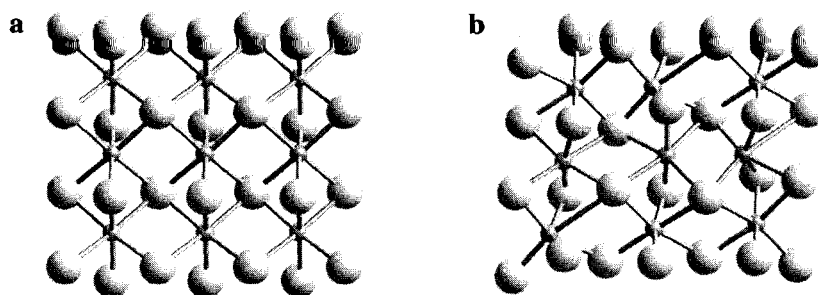


Figure 10. Structures of FeS II (a) and FeS III (b). Both are distorted versions of the NiAs structure.

have a dodecahedral shape. Most garnets display cubic symmetry, however majorite can be tetragonal because of ordering of the two octahedral cations.

Studies of garnet crystal structures at high-pressures by single crystal diffraction have been published on pyrope, grossular, and andradite (Hazen and Finger 1978, 1989; Levien et al. 1979). These studies conclude that the compression of garnets is controlled by the compressibility of the dodecahedral site. For example, the bulk modulus of andradite is 159 GPa and its dodecahedral cation, Ca, has a bulk modulus of 160 GPa. Thus the collapse of the framework, or other words, the tilting of the tetrahedra and octahedra into the dodecahedral site, accomplishes compression.

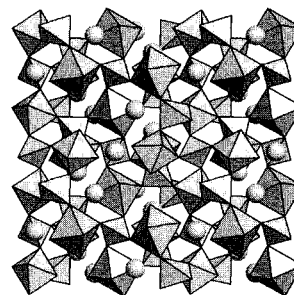


Figure 11. Structure of majorite viewed down the *c* axis displaying a depth of 1/2 of the unit cell. The small octahedra represent SiO₆ groups, while the larger represent MgO₆ groups. A sphere represents the dodecahedral atoms.

However, in a study of the comparative compressibilities of garnets Hazen et al. (1994) demonstrated that this model does not hold for the majorite type garnets. A garnet with Na in the dodecahedral site was found to be the least compressible garnet ever measured and yet the compressibility of Na is quite high. It was suggested in this study that the compressibility of garnet might, in fact, be controlled by octahedral-O-tetrahedral angle bending, which in turn is modified by bonding of the dodecahedral cation. This is quite analogous to the compressibility mechanism observed for the feldspars. We must conclude that the details about garnet compressibilities need further work.

Spinel

The formula for the spinel type structure is B_2AO_4 . Examples are spinel, Al_2MgO_4 , magnetite, Fe_3O_4 , and ringwoodite, Mg_2SiO_4 . The oxygen anions are in a cubic closest-packed arrangement with the *B* cation in octahedral sites and the *A* cation in tetrahedral. The octahedra form edge-sharing chains that are linked together by the isolated tetrahedra. All atoms are in special positions, and the only variables for the structure are the cubic cell edge

and the x position of the oxygen atom. The cell edge can be determined from the octahedral, R_O , and tetrahedral, R_T , bond lengths as

$$a = \frac{40 R_T + 8 \sqrt{33R_O^2 - 8 R_T^2}}{11 \sqrt{3}}.$$

This means that compression of the structure “depends” only on the compressibility of the tetrahedral and octahedral bonds. The compression behavior can be separated into 3 categories based on bond compressibilities: (1) the compressibilities of the two bonds are equal, (2) R_T is softer than R_O , (3) R_O is softer than R_T (Finger et al. 1986).

Magnetite offers a good example of a structure with bonds that are roughly equal in strength. This structure compresses primarily by scaling until it transforms to the marokite, CaMn_2O_4 , structure with Fe^{3+} in octahedral coordination and Fe^{2+} in 8-fold coordination (Fei et al. 1998). The transformation at a pressure near 25 GPa was first reported by Mao et al. (1974). Huang and Bassett (1986) determined a slope of $-68^\circ\text{C}/\text{GPa}$ for the phase boundary. The crystal structure of magnetite to 4.5 GPa has been determined by Finger et al. (1986) and recently to 30 GPa by Haavik et al. (1998). There has been a wide range of values (190-220 GPa) determined for the bulk modulus, with 220 GPa the latest value reported by Haavik et al. (1998).

The mineral spinel is an example of a structure with soft tetrahedral bonds (Mg-O) and stronger octahedral bonds (Al-O). Its structure has been determined by Finger et al. (1986) to 4.0 GPa and more recently by Pavese et al. (1998) to 3.8 GPa in their study of cation partitioning as a function of P . The result of a softer tetrahedral bond is that the tetrahedra compress more rapidly than the octahedra. Consequently the octahedral site undergoes distortion that increases the length of the shared octahedral edge. In terms of Pauling's rules this leads to a destabilization of the structure. Liu (1975, 1980) demonstrated that Al_2MgO_4 spinel decomposes to a mixture of MgO and Al_2O_3 at pressures above 15 GPa. However, with temperatures above 1000°C and P above 25 GPa, Irifune et al. (1991) observed that Al_2MgO_4 adopts the CaFe_2O_4 calcium ferrite structure. This structure is a slight modification of the marokite structure adopted by Fe_3O_4 at high pressure. The bulk modulus was determined as 190-194 GPa with $K'_O = 4$ by diffraction techniques, and 198 GPa by Brillouin spectroscopy (Askarpour et al. 1993). In more recent work using a combination of synchrotron x-ray diffraction with a diamond cell up to pressures of 70 GPa, Funamori et al. (1998) found that MgAl_2O_4 spinel transforms first to Al_2O_3 plus MgO, then to the CaFe_2O_4 phase, and finally to a new phase having the CaTi_2O_4 structure above ~ 40 GPa.

As an example of a spinel structure with tetrahedral bonds that are stronger than the octahedral ones, we can look at Ni_2SiO_4 . The structure was determined by Finger et al. (1979) to 3.8 GPa. They found that the Si-O bond did not vary but the Ni-O bond decreased, as we would predict. Over a given volume decrease the distortion of the octahedral site is much less with this type of spinel than for one with weak tetrahedral bonds. Therefore this structure should be more stable than the one with weak tetrahedral bonds.

The most important spinels as far as the Earth's interior is concerned are the $(\text{Mg,Fe})_2\text{SiO}_4$ spinels. The only known natural occurrence of a $(\text{Mg,Fe})_2\text{SiO}_4$ spinel is in a meteorite (ringwoodite, Fig. 12), but it is thought to be a major phase in the transition zone. Hazen (1993) collected compressibility data for five different chemistries along the Fe-Mg join. He found that the Mg_2SiO_4 spinel had a $K_O = 184$ GPa, while Fe_2SiO_4 spinel had a $K_O = 207$ GPa. This was taken as a demonstration that although Fe and Mg appear to

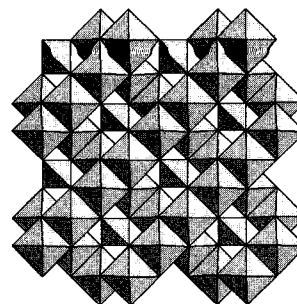


Figure 12. Structure of ringwoodite viewed down the c axis displaying a depth of $1/4$ of the unit cell. Note the diagonal crisscrossing chains of MgO_6 octahedra linked together by isolated SiO_4 tetrahedra.

be similar at room conditions, they behave differently at higher pressures. Zerr et al. (1993) studied the compressibility of $(\text{Mg}_{0.6}\text{Fe}_{0.4})_2\text{SiO}_4$ spinel to 50 GPa and obtained $K_0 = 183.0$ GPa, $K' = 5.4$. Irifune et al. (1998) determined the phase boundary for Mg_2SiO_4 spinel in the temperature range of 1400-1800°C and found a negative dT/dP with a transformation pressure of 21 GPa at 1600°C. This spinel transforms to $\text{MgO} + \text{MgSiO}_3$ perovskite.

Wadsleyite

The mineral known as wadsleyite was first synthesized by Ringwood and Major (1966) who were exploring the Mg_2SiO_4 - Fe_2SiO_4 spinel solid solutions at pressures up to 17.5 GPa and temperatures of 1500°C. They were successful in making cubic spinel crystals in compositions containing about 20% Fe and higher, but the product for the Mg_2SiO_4 end member was birefringent and thus of a lower symmetry than cubic. Their conclusion was that this was a new phase and they thought it might be a quench product, i.e., it had the spinel structure under the synthesis conditions but distorted to a lower symmetry upon quenching. It turns out, of course, that they made a new structure that is intermediate in its pressure range between forsterite and ringwoodite. Until this phase was reported as occurring in the Peace River meteorite by Price et al. (1983), it was called by a variety of names including “modified spinel,” “beta phase,” “beta spinel,” and, more rarely, “ β - Mg_2SiO_4 .” All of these terms except the latter are examples of very poor usage because the phase is really different from spinel and is not just a simple distortion of the spinel structure. Price et al. (1983) followed the suggestion of Ringwood that it be named for David Wadsley, a well-known Australian mineralogist and crystallographer. The structure of orthorhombic wadsleyite is given in Figure 13. The structure in this orientation is made of two kinds of layers, one that just contains MgO_6 octahedra plus vacant sites and another that contains MgO_6 octahedra and SiO_4 tetrahedra plus vacant sites. In some respects it is like the hydrous magnesium silicates discussed in the next section and this may be related to the fact that wadsleyite synthesized in the presence of H_2O can

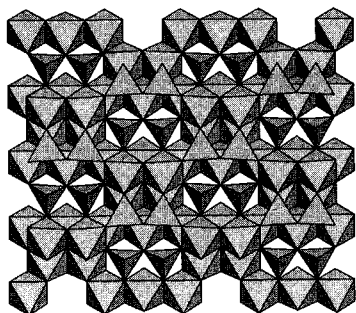


Figure 13. Structure of wadsleyite viewed down $[201]$ showing 2 layers of polyhedra. The lower layer is composed only of octahedra and the upper layer is a mix of tetrahedra and octahedra.

accommodate up to about 3.3% H₂O (Smyth 1994). Smyth and others propose that wadsleyite is a candidate for being a major reservoir for H₂O in Earth's transition zone. In addition to the orthorhombic phase mentioned above, Smyth et al. (1997) described a related monoclinic structure that apparently results from a particular kind of cation ordering.

Dense hydrous magnesium silicates

Water (hydrogen) is stored in the upper mantle in hydrous silicate minerals such as amphibole, phlogopite, and serpentine. High-pressure and high-temperature experiments have shown that such minerals are stable to depths of ~200 km, but at greater depths they decompose and the water contained in them is released. Experimental studies of hydrous magnesium silicates over the past 25 years have demonstrated the existence of a number of hydrous phases with stabilities corresponding to depths much greater than 200 km. If present in the mantle, such materials would have a very significant effect on properties because virtually all mantle models are based on anhydrous minerals such as olivine, spinel, garnet, and silicate perovskite. There is, however, considerable confusion over the nomenclature and identification of these materials because many experimental runs result in multi-phase and/or very fine-grained products.

Figure 14. Ternary diagram showing compositions of hydrous magnesium silicates.

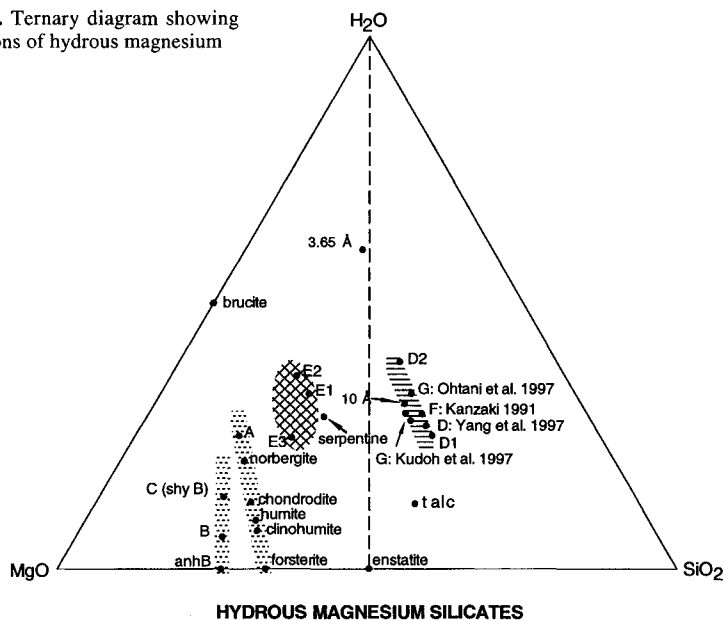


Figure 14 is a ternary diagram that shows the compositions of various hydrous magnesium silicates that either occur as minerals or have been synthesized in the laboratory. The ones containing octahedral Si, such as phases B, superhydrous B, and phase D are often called dense hydrous magnesium silicates (DHMS). The nomenclature of these high-pressure phases is based on either a description of a prominent line in the x-ray pattern or by an alphabetic naming scheme. The phases described thus far include the 10 Å phase (Sclar et al. 1965a,b), the 3.65 Å phase (Sclar et al. 1967), phases A, B, and C (Ringwood and Major 1967b), D (Yamamoto and Akimoto 1974), D' (Liu 1987), E (Kanzaki 1989 1991), F (Kanzaki 1991), anhydrous B (Herzberg and Gasparik 1989), and superhydrous B (Gasparik 1990). Crystal structure investigations of phases B and anhB

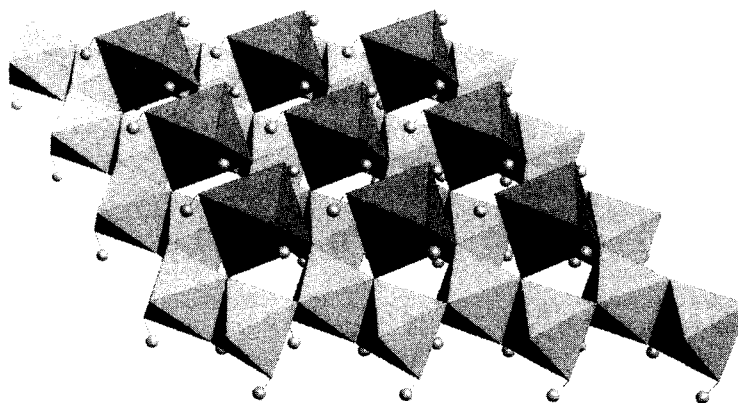


Figure 15. Structure of phase D. One layer contains Mg ions occupying 1/3 of the possible octahedral sites and the other layer contains Si ions occupying 2/3 of the possible octahedral sites.

(Finger et al. 1989 1991) illustrate how hydrogen is incorporated into phase B and how reliable crystal structure information is essential for interpretation of complex high-pressure phase chemistry. No crystal structures have been reported for the 10 Å phase or the 3.65 Å phase, and no authors other than Sclar et al. (1965a) have reported the existence of the latter. The 10 Å phase has been synthesized in polycrystalline form by several investigators and it is thought that its structure is similar to that of talc.

Phase C is probably identical to superhydrous B, an identity that was obscured for many years because the product used for the diffraction pattern of Ringwood and Major (1967b) was not a single phase and the pattern itself was not of high quality. Yamamoto and Akimoto's (1974) phase D turned out to be chondrodite, one of the humite series, but another synthetic product named phase D (Liu 1987) is potentially the most important of these materials because it has the highest pressure stability of any of the DHMS family. The crystal structure of phase D was described by Yang et al. (1997) and is shown in Figure 15. It has the same crystal structure as that of phase G reported by Kudoh et al. (1997) and its high pressure-temperature stability is discussed in several papers (Ohtani et al. 1997, Frost and Fei 1998, Shieh et al. 1998).

Kanzaki (1991) and Kudoh et al. (1995) described the synthesis and characterization of phase F, but it appears that the material reported by Kanzaki (1991) as phase F is actually phase D, and Kudoh et al.'s (1995) phase F is misindexed phase C, i.e. misindexed superhydrous phase B. Kudoh et al. (1997) recognized this error and withdrew their 1995 paper on phase F.

Phase E has a very unusual crystal structure that apparently is characterized by long-range disorder (Kudoh et al. 1989 1993), but is unusual in that its single-crystal diffraction pattern shows sharp spots with no evidence of disorder. Liu et al. (1997) characterize phase E as "the hydrous form of forsterite," but additional work is needed to determine whether this observation is valid or whether the quenched phase E has the same structure as under the original synthesis conditions.

Although several hydrous magnesium silicates such as anthophyllite, serpentine, talc, and the humites are well-known minerals, the synthetic phases are of considerable interest because at least some of them appear to be stable at substantially higher pressures and temperatures than the minerals. Whether or not any of these phases occur naturally is still an open question, but their study does provide a framework in which investigators can

develop models that incorporate H_2O , $(\text{OH})^+$, or H^+ as essential constituents of the phase chemistry. Furthermore, development of the crystal chemistry provides important information on the transformation of Si coordination from four to six with increasing pressure and on structural features that permit hydrogen to be retained under extreme conditions. Ahrens (1989) discusses how water was introduced into the Earth and how it might be stored in the mantle over geological time. He points out that it is unlikely that substantial amounts of water are re-introduced to the mantle through subduction processes, but current ideas suggest that a considerable amount of water is present as a result of the early stages of the Earth's accretion. This water has been released through time to form and replenish the oceans, lakes, rivers, and other repositories of water in the crust. An alternate view of how hydrogen might be incorporated into phases stable in the mantle is presented in papers, for example, by Rossman and Smyth (1990), Skogby et al. (1990), McMillan et al. (1991), and Smyth (1987). These authors have identified minute, but significant, amounts of structural hydrogen in nominally anhydrous minerals such as pyroxene and wadsleyite. Their idea is that if the amount of hydrogen found in these phases is representative of the mantle, then a volume of water equivalent to several times that of the present oceans could be generated and thus there is no reason to invoke the presence of hydrous magnesium silicates stable only at high pressures. Currently, we have no evidence to prove or disprove either model, but information being provided in both areas can be used to support further investigations.

Pyroxenes

Pyroxenes are significant phases in the upper mantle and occur in several space groups and compositional ranges. Pyroxene structures are comprised of slabs of octahedra extending along the c axis and connected top, bottom, left, and right to other octahedral slabs by single tetrahedral chains. Orthopyroxene, $(\text{Mg,Fe})\text{SiO}_3$, shown in Figure 16 usually contains a small amount of Ca and crystallizes in space group $Pbca$. There are three clinopyroxene structures stable at relatively moderate pressures, clinopyroxene, $(\text{Mg,Fe})\text{SiO}_3$, with space group $P2_1/c$ (Fig. 17), several different compositions with space group $C2/c$, diopside-hedenbergite [$\text{Ca}(\text{Mg,Fe})\text{Si}_2\text{O}_6$], augite $\text{Ca}(\text{Mg,Fe,Al})\text{Si}_2\text{O}_6$, and jadeite ($\text{NaAlSi}_2\text{O}_6$ —Fig. 18), and omphacite, whose ideal composition is 50% jadeite and 50% diopside, but with a different space group, $P2/n$. Recently, however, a high-pressure transition from $P2_1/c$ clinoenstatite to a $C2/c$ clinoenstatite was predicted by Pacalo and Gasparik (1990) and confirmed by Angel et al. (1992). The implication of this is that a phase transition from low-P to high-P clinoenstatite could be responsible for the “X-discontinuity” observed in some seismic profiles at about 300 km depth (Woodland 1998).

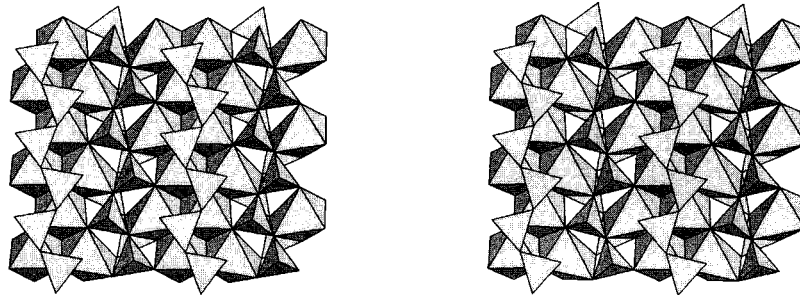


Figure 16 (left). Structure of orthoenstatite looking down the a axis at a depth of 0.0–0.3. The c axis parallels the direction of the chains. The $M2$ site is located in the more distorted octahedra.

Figure 17 (right). Structure of clinoenstatite with the same orientation and depth as for orthoenstatite.

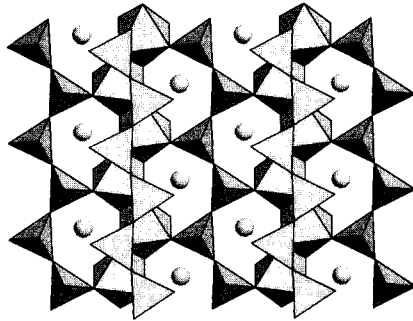


Figure 18. Structure of jadeite with the same orientation and depth as for orthoenstatite.

A similar result was obtained by Yang et al. (1998), who pressurized a single crystal of protopyroxene with composition $(\text{Mg}_{1.54}\text{Li}_{0.23}\text{Sc}_{0.23})\text{Si}_2\text{O}_6$ and space group $Pbcn$ in a diamond cell and observed a room-temperature transition between 2.03 and 2.50 GPa to a structure with space group $P2_1cn$. Even though this is a reconstructive, first-order transition, it takes place at room temperature and is reversible with a ΔV for the transition of 2.6%. Interestingly, no indication of a reconstructive phase transition has been observed in orthopyroxene, although Hugh-Jones and Angel (1994) did note a change in slope of O3-O3-O3 angles at about 4 GPa, indicating that some structural adjustment was taking place as the pressure increased. As can be seen in the phase diagram of Figure 1, further increases in pressure result in MgSiO_3 pyroxenes transforming to garnet or ilmenite, depending on the temperature and pressure involved.

Olivine

Olivine is one of the most important minerals in the upper mantle, along with pyroxenes and garnets. The geologically relevant end-member phases are forsterite (Fo), Mg_2SiO_4 , and fayalite (Fa), Fe_2SiO_4 with the natural composition being somewhere near $\text{Fo}_{90}\text{Fa}_{10}$. The transformation of olivine to wadsleyite is widely accepted as the source of the discontinuity that is observed in seismic velocities at 410-km depth (Bernal 1936).

The structure of forsterite (Fig. 19) is based on a distorted hexagonal closest-packed array of oxygen atoms with 1 tetrahedral site (T) and 2 non-equivalent octahedral sites (M_1 , M_2). The M_1 site is more distorted than the M_2 site largely because the M_1 octahedron shares 6 of its edges with neighboring polyhedra (2 with M_1 , 2 with M_2 and 2 with T) while the M_2 octahedron only shares 3 edges (2 with M_1 , and 1 with T). According to Pauling's rules, shared edges are shorter than unshared edges in order to screen cation-cation repulsion. Much research has been directed to understanding olivine structural systematics and the reader is directed to "Orthosilicates," *Reviews in Mineralogy*, Volume 5 for an in-depth discussion.

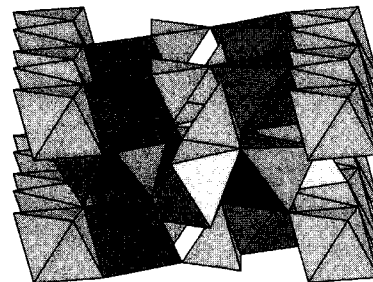


Figure 19. Structure of forsterite with the b axis horizontal and the c axis parallel to the chains of octahedra, coming out of the page. The illustration include the portion of the structure within the volume defined by $[(-0.2 - 1.2)x, (-0.2 - 1.2)y, (-0.5 - 1.5)z]$. The M_2 octahedra are the distorted ones.

Because of the importance of olivine at depth there have been quite a few studies of its compressibility. For example, Olinger, (1977), Kudoh and Takéuchi, (1985), Will et al. (1986), Andrault et al. (1995), Downs et al. (1996) all studied the compressibility of various olivines by determining the cell parameters as a function of pressure, obtaining a value for the bulk modulus around 120-130 GPa. All have found that the compression is anisotropic with the compressibilities of the cell edges ($\beta_a = (1/a)(da/dP)$, etc.) of a , b , and c to be 1.35, 2.70, and $2.10 \times 10^{-3} \text{ GPa}^{-1}$, respectively (Downs et al. 1996). It follows that the relative axial ratios are 1:1.99:1.55 for $a:b:c$. Kinks in the compressibility curves of the cell edges were reported by Kudoh and Takéuchi (1985), and confirmed by Will et al., (1986) as well as in Raman and infrared spectroscopic studies (Chopelas 1990, Wang et al. 1993, Durben et al. 1993). These studies interpreted the change as an indication of a second-order phase transition or a change in the compression mechanism of forsterite at 10 GPa. However, Downs et al. (1996) suggested that errors may have been introduced in the data sets for these studies because they all used 4:1 methanol:ethanol as a pressure medium and it freezes at pressures near 10 GPa. No deviation from a smooth trend was observed in the Downs et al. (1996) study, which used He as a pressure medium. The smooth trends have also been observed in the state-of-the-art Brillouin experiments on both forsterite and San Carlos olivine to 16 and 32 GPa, respectively (Zha et al. 1996, 1998).

Crystal structures of olivines as a function of pressure have been determined for forsterite (Hazen 1976, Hazen and Finger 1979, Kudoh and Takéuchi 1985), fayalite (Hazen 1977, Kudoh and Takeda 1986), monticellite MgCaSiO_4 (Sharp et al. 1987), chrysoberyl Al_2BeO_4 (Hazen 1987) and LiScSiO_4 (Hazen et al. 1996). The anisotropy in the compression of olivine was shown to be chemistry dependent (Hazen et al. 1996) with the a -axis compression controlled by the stacking of M1 and T columns, and b and c controlled by the compressibility of the M2 octahedron. Therefore, a structure such as LiScSiO_4 ends up quite isotropic because soft Li are in M1, while stiff Sc are in the M2 site.

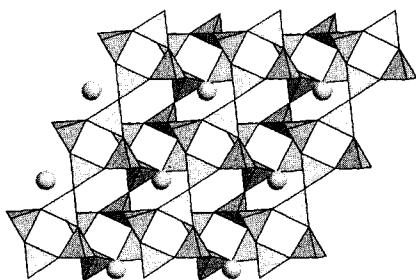


Figure 20. Structure of albite viewed down the b axis. The c axis parallels the chains of four-membered rings. The Na atoms are indicated by spheres. The image includes the volume bounded by $[(-1.0 - 2.0)x, (0.0 - 0.5)y, (-1.0 - 2.0)z]$.

Feldspars

The feldspar group of minerals is the most important of the crustal phases because it makes up about 50-60% of its total volume. The major phases are albite, $\text{NaAlSi}_3\text{O}_8$, K-spar (microcline, orthoclase, sanidine) KAlSi_3O_8 , and anorthite $\text{CaAl}_2\text{Si}_2\text{O}_8$. The crystal structures of all the feldspars show similar topology, effectively shown in Figure 20 viewed along $[010]$. The structure can be considered as made of four-membered tetrahedral rings that are linked together to form chains that run parallel to the c -axis. These chains form layers that are separated by channels. The layers are stacked with chains over chains to form pairs, and each pair is shifted to be over the channels of the adjoining pairs. The Na, K, and Ca atoms occupy the channels situated between layers within the pairs.

Single crystal high-pressure structural studies have been completed for low albite (Downs et al. 1994), microcline (Allan and Angel 1997), anorthite (Angel 1988) and reedmergnerite, NaBSi_3O_8 (Downs et al. 1998) with bulk moduli of 55, 60, 80, and 69 GPa, respectively. All feldspars display anisotropic compression, with maximum compressibility coinciding with the narrowing of the channels. Each structure compresses by bending of the $T\text{-O-T}$ angles, with some getting smaller and some getting larger, leaving the strongly bonded tetrahedra unchanged. On one hand, albite and reedmergnerite compress by bending the O_cO angle which narrows the channel and causes the chains in different layers to slide over each other. On the other hand, microcline accomplishes the channel narrowing by shearing the four-membered rings. Downs et al. (1998) suggest that the typical framework $T\text{-O-T}$ angle bending mechanism is being perturbed by the bonding of the Ca, K, and Na atoms. Consequently, even though each $T\text{-O-T}$ angle in anorthite is Al-O-Si, which is softer than Si-O-Si, each of these bridging O atoms is also bonded to one or two Ca atoms. The Ca-O distance (2.48 Å) is shorter than R(K-O) (2.89 Å) and the same as R(Na-O) (2.49 Å), but every O atom is bonded to Ca, so it stiffens the Al-O-Si angles to the extent that anorthite is the least compressible of the feldspars. Albite, reedmergnerite and microcline have the same Al,Si distribution but electron density calculations show that the smaller Na atom is bonded to only 5 oxygens, while K is bonded to seven (Downs et al. 1996). The O_cO atom in low-albite is not bonded to Na and so the Al- O_cO -Si angle is unconstrained and compresses with the little force. Therefore albite has the smallest bulk modulus. Reedmergnerite compresses similarly to albite because of similar Na-O bonding, but with a larger bulk modulus because B-O-Si angles are stiffer than Al-O-Si. The O_cO atom in microcline is bonded to K, and this stiffens the structure. This explains why the bulk modulus of microcline is larger than that of albite, in spite of the fact that the unit cell of microcline is significantly larger than that of albite.

Hollandite

Hollandite is a structure-type named after the mineral $\text{BaMn}_8\text{O}_{16}$ whose structure is indicated in Figure 21. It is constructed of edge-sharing octahedra that form a four-sided eight-membered channel that is capable of containing a low-valence large-radius cation. Together the O atoms and the large cation form a hexagonal closest packed structure, a sort of analogue to the cubic closest packed perovskite. The similarity of the structure to stishovite should remind one of the similarities of coesite and the feldspars. The structure is of considerable interest to the nuclear waste and ion diffusion communities.

Ringwood et al. (1967) transformed sanidine at 900°C and 12 GPa into the hollandite structure with Al and Si randomly occupying the octahedral sites. This was the first oxide structure identified with both Al and Si displaying sixfold coordination and only the

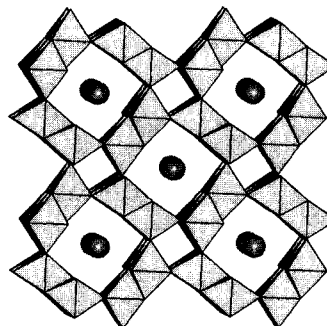


Figure 21. Structure of hollandite viewed down the c axis, with $\pm 1/2$ unit cell in the a - b plane.

second, after stishovite, with ${}^6\text{Si}$. They postulated that because feldspars are the most abundant minerals in the Earth's crust, it is possible that the hollandite structure with ${}^6\text{Al}$ and ${}^6\text{Si}$, may be a common phase within the transition zone of the mantle. Subsequently, Reid and Ringwood (1969) systematically examined the feldspar structure type materials to identify others that would transform to the hollandite structure at high pressures. They were able to synthesize $\text{Sr}_x\text{Al}_{2x}\text{Si}_{4-2x}\text{O}_8$ and $\text{Ba}_x\text{Al}_{2x}\text{Si}_{4-2x}\text{O}_8$, $x \sim 0.75$ with the hollandite structure, but failed with the Na, Ca, and Rb rich feldspars. Yamada et al. (1984) determined the structure of the KAlSi_3O_8 phase by powder diffraction methods and Zhang et al. (1993) reported the structure as a function of pressure.

Madon et al. (1989) reported that their synthesis of $(\text{Ca}_{0.5}\text{Mg}_{0.5})\text{Al}_2\text{Si}_2\text{O}_8$ at 50 GPa and laser-induced high temperatures exhibited an x-ray powder diffraction pattern consistent with hollandite. Liu (1978) reported the synthesis of $\text{NaAlSi}_3\text{O}_8$ hollandite at 21-24 GPa from jadeite plus stishovite. Above 24 GPa the $\text{NaAlSi}_3\text{O}_8$ hollandite transforms to the calcium ferrite structure. Gasparik (1989) synthesized an unknown purple phase in an anvil press from a starting mixture of jadeite, orthoenstatite, and orthopyroxene $\text{En}_{44}\text{Py}_{56}$ at 1450°C and 16.5 GPa with a Pb flux. Downs et al. (1995) determined this to be a hollandite structure of composition $\text{Pb}_{0.8}\text{Al}_{1.6}\text{Si}_{2.4}\text{O}_8$. It thus seems that aluminosilicate hollandite is capable of containing many of the large low valence cations at elevated temperatures and pressures.

REFERENCES

- Ahrens TJ (1989) Water storage in the mantle. *Nature* 342:122-123
- Allan DR, Angel RJ (1997) A high-pressure structural study of microcline (KAlSi_3O_8) to 7 GPa. *Eur J Mineral* 9:263-275
- Anderson OL (1997) Iron: beta phase frays. *Science* 278:821-822
- Andrault D, Bouhifd MA, Itié JP, Richet P (1995) Compression and amorphization of $(\text{Mg,Fe})_2\text{SiO}_4$ olivines: an x-ray diffraction study up to 70 GPa. *Phys Chem Minerals* 22:99-107
- Angel RJ (1988) High-pressure structure of anorthite. *Am Min* 73:1114-1119
- Angel RJ, Allan DR, Miletich R, Finger LW (1997) The use of quartz as an internal pressure standard in high-pressure crystallography. *J Appl Cryst* 30:461-466
- Angel RJ, Chopelas A, Ross NL (1992) Stability of high-density clinoenstatite at upper-mantle pressures. *Nature* 358:322-324
- Angel RJ, Ross NL, Seifert F, Fliervoet TF (1996) Structural characterization of pentacoordinate silicon in a calcium silicate. *Nature* 384:441-444
- Askarpour V, Manghnani MH, Fassbender S, Yoneda A (1993) Elasticity of single-crystal MgAl_2O_4 spinel up to 1273 K by Brillouin spectroscopy. *Phys Chem Minerals* 19:511-519
- Bernal JD (1936) *The Observatory* 59:268
- Besson JM, Nelmes RJ, Hamel G, Loveday JS, Weill G, Hull S (1992) Neutron powder diffraction above 10-GPa. *Physica B* 180:907-910
- Bloss FD (1994) *Crystallography and Crystal Chemistry*. Mineralogical Society of America, Washington, DC, 545 p
- Boehler R, von BN, Chopelas A (1990) Melting, thermal expansion, and phase transitions of iron at high pressures. *J Geophys Res* 95:21731-21736
- Boisen MB Jr, Gibbs GV (1993) A modeling of the structure and compressibility of quartz with a molecular potential and its transferability to cristobalite and coesite. *Phys Chem Minerals* 20:123-135
- Buerger MJ (1961) Polymorphism and phase transformations. *Fortschr Mineral* 39:9-24
- Chopelas A (1990) Thermal properties of forsterite at mantle pressures derived from vibrational spectroscopy. *Phys Chem Minerals* 17:149-156
- Downs RT, Andalman A, Hudacsko M (1996) The coordination numbers of Na and K atoms in low albite and microcline as determined from a procrystal electron-density distribution. *Am Mineral* 81:1344-1349
- Downs RT, Hazen RM, Finger LW (1994) The high-pressure crystal chemistry of low albite and the origin of the pressure dependency of Al-Si ordering. *Am Mineral* 79:1042-1052
- Downs RT, Hazen RM, Finger LW, Gasparik T (1995) Crystal chemistry of lead aluminosilicate hollandite: a new high-pressure synthetic phase with octahedral Si. *Am Mineral* 80:937-940
- Downs RT, Palmer DC (1994) The pressure behavior of α -cristobalite. *Am Mineral* 79:9-14

